Molecular Structure and Properties of Click Hydrogels with Controlled Dangling End Defect

Ao-kai Zhang[1,2], Jun Ling[3], Kewen Li[1], Guo-Dong Fu[,1], Tasuku Nakajima[4], Takayuki Nonoyama[4], Takayuki Kurokawa[4], Jian Ping Gong*[,4]*

[1]School of Chemistry and Chemical Engineering, Southeast University, Jiangning District, Nanjing, Jiangsu Province, P. R. China 211189

[2]Graduate School of Life Science, Hokkaido University, Sapporo, 060-0810, Japan

[3]Department of Polymer Science and Engineering, Zhejiang University, Hangzhou, P. R. China 310027

[4]Faculty of Advanced Life Science, Hokkaido University, Sapporo, 060-0810, Japan

ABSTRACT

In this study, controlled amount of dangling ends is introduced to the two series of poly(ethylene glycol)-based hydrogel networks with 3 and 4 cross-linking functionality by using click chemistry. The structure of the gels with regulated defect percentage is confirmed by comparing the results of low-field NMR characterization and Monte Carlo simulation. The mechanical properties of these gels were characterized by tensile stress-strain behaviors of the gels, and the results are analyzed by Gent model and Mooney-Rivlin model. The shear modulus of the swollen gels is found to be dependent on the functionality of the network, and decreases with the defect percentage. Furthermore, the value of shear modulus well obeys the phantom model for all the gels with varied percentage of the defects. The maximum extension ratio, obtained from the fitting of Gent model, is also found to be dependent on the functionality of the network, and does not change with the defect percentage, except at very high defect percentage. The value of the maximum extension ratio is between that predicted from phantom model and the affine model. This indicates that at the large deformation, the fluctuation of the cross-linking points is suppressed for some extend but still exists. Polymer volume fractions at various defect percentages obtained from prediction of Flory-Rehner model are found to be in well agreement with the swelling experiment. All these results indicate that click chemistry is a powerful method to regulate the network structure and mechanical properties of the gels.

KEYWORDS: Hydrogel, Click chemistry, Dangling ends, Network inhomogeneity, Monte Carlo simulation, Mechanical property, Gent model, Phantom model, affine model

Introduction

Polymer hydrogels, which usually contain more than 90 % water, has been widely used in tissue engineering,[1,2] drug delivery systems[3,4] and superabsorbent materials.[5,6] The mechanical properties of hydrogels are determined by microscopic network structure, the latter is considered to be greatly influenced by network defects (inhomogeneities).[7] Network defects can be mainly classified as spatial and topological defects.[8] The spatial defect refers to the nonuniform distribution of cross-linkers. The topological defects include entanglements, loops, and dangling ends. Among them, loops and dangling ends are inelastic part under deformation, while entanglements are a major account for a higher modulus in experiment than in phantom prediction.[9] All of them lead to a deviation in gel structure from the "ideal" network.[10] Many innovative works aimed to regulate gel properties by controlling network structures. Most of them attempted to minimize network defects, for example, by cross-end coupling of two tetra-arm pre-polymers at the overlap concentration,[11] or by introducing movable "figure of eight" cross-linkers that can maintain network homogeneity upon deformation.[12] On the contrary, a "double network" concept was applied to achieve extremely tough hydrogels by manually introducing network inhomogeneities.[13] However, there exist few works on precisely regulating gel properties by network topological defects,[14] although it fits the object to broaden the engineering application and elasticity theory of hydrogels. The reason may be the shortage of robust synthesis and characterization methods that can precisely introduce and characterize network topological defects in gel networks.

Click chemistry,[15,16] which has a high reaction efficiency and high atom economy (~100 %), has been successfully used to prepare model network of precise structure and controllable properties.[17-21] UV and fluorescence analysis indicated that only a maximum of 0.2 % unreacted

functional groups remained after initial gel formation.[21] The quantitative coupling nature makes it an encouraging alternative to other reactions in hydrogel preparing.[22,23] To better control the reaction rate and obtain a homogeneous gel, an improved CuAAc method[24] using thermal initiation to reduce Cu(II) to Cu(I) was used in this work. Among the state-of-art method to characterize gel network structure such as multiple-quantum (MQ)NMR,[25-27] small-angle X-ray (SAXS) or neutron scattering (SANS)[28-30], and network disassembly spectrometry (NDS),[31,32] the low-field solid NMR is a powerful tool for its ability in distinguishing topological defect from elastic network chains by their different chain mobility.[33,34] Monte Carlo (MC) simulation[35,36] has been proved to be a robust tool in the study of polymer network formation, structure, and dynamics.[37-39] The simulation method can shed light on the microscopic network structures which are not experimentally accessible.

In this study, the effect of dangling ends defect on gel properties was investigated. Precise amount of dangling ends were introduced by replacing original multi-functional cross-linkers with mono-azide-functional molecules, while maintaining functional group stoichiometry. Network structure parameters such as gel fraction and elastic fraction were characterized by leach experiment, low-field NMR and Monte Carlo simulation. Mechanical properties and swelling ratio of click gels with various content of random defect were characterized by tensile test and swelling test, respectively. The shear modulus and the maximum tensile stretching ratio were obtained by analyzing the experimental data using Gent model. The mechanical behaviors are discussed and compared with the phantom model and affine model. The swelling results are quantitatively compared with the Flory-Rehner model.

Experimental

Materials and synthesis

Propargyl bromide (80%), PEG (M_n = 2000 g/mol), and pentamethyldiethylenetriamine (PMDETA, 99 %) were purchased from Aldrich Chemical Co.. $CuBr_2$ (99 %), pentaerythritol and sodium azide (99 %) were purchased from Shanghai Chemical Reagent Plant. 1,1,1-Tris(hydroxymethyl)ethane and 3-Methyl-1-pentyn-3-ol (B_1) were purchased from Acros Organic Co. of Geel, Belgium. Azobisisobutyronitrile (AIBN) was purchased from Wako Co.. All the chemicals were used directly without further purification.

The synthesis of tetrakis(2-propynyloxymethyl)methane (B_4) is the same as described by L. Q. Xu et al..[17] The synthesis of 3-[2,2-Bis(prop-2-ynyloximethyl)propyloxy]prop-1-yne (B_3) reagent is the same as described by Gragert[40] and Schunack.[41] The synthesis of α, ω-diazido PEG2k (A_2) is the same as used by G. D. Fu et al..[42]

Preparation of click hydrogels

Determination of *c.** To optimize the synthesis condition and reduce the probability of forming entanglement, the gel was prepared at a relative dilute pre-polymer concentration near the overlap concentration (c^*) of PEG2k/DMF which is determined by viscosity,[43] and described in Supporting Information (Fig. S1). The calculated R_g^2 and c^* for PEG2k/DMF are 229.6 nm^2 and 239.29 g/L, respectively.

Gel preparation.

Single network click gels without or with controlled amount of dangling ends defect were prepared by thermal initiated CuAAC end-linking reaction between difunctional polymer skeleton A_2 and multi-functional cross-linkers B_f (functionality f=3, 4) in the presence of dangling ends forming molecules B_1 with equimolar concentration of functional groups of A and B(azide : alkyne = 1 : 1). The molar ratio of alkyne group ended multifunctional cross-linkers B_f

(*f*=3, 4) and B_1 are varied (Scheme 1). The defect percentage is defined as X_{exp} (%) = 100 × B_1(mol)/[B_f (mol)+ B_1(mol)]. *f* functional gels with X % of dangling ends defect were denoted as G*f*-X. For a typical fabrication procedure, 0.1 g of A_2, certain amount of B_1 and B_f was added to a glass bottle, while maintaining the stoichiometry of A and B groups. Then, $CuBr_2$ (2.5×10^{-5} mol), AIBN (4.5×10^{-5} mol), PMDETA (2×10^{-6} mol) and certain amount of DMF were added to the pre-reaction solution and mixed, with a concentration of pre-polymer solution at overlap concentration of PEG2k/DMF (239.29 g/L). After that, the solution was poured to a reaction cell consisting of two glass plates with a spacer and heated in an oven at 60 °C. At least 6 h were allowed for the completion of cross-linking reaction.

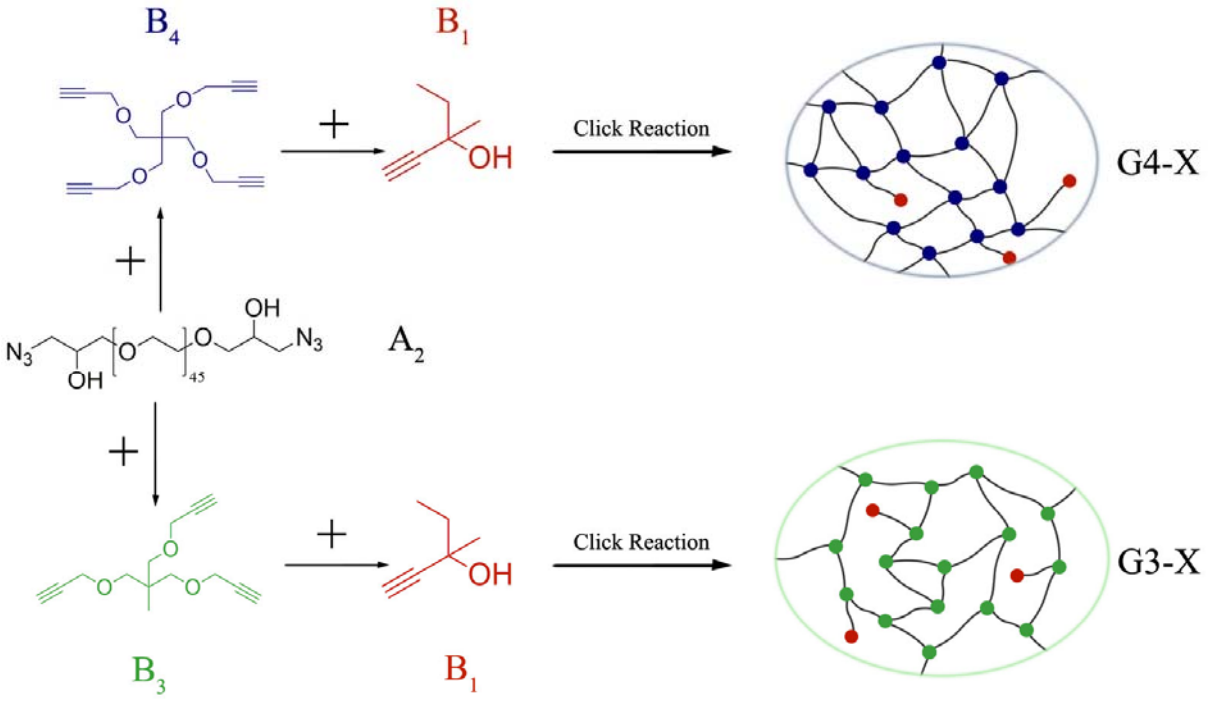

Scheme 1. Preparation of 4 functional network G4 and 3 functional network G3 with controlled amount of dangling ends using click chemistry.

Determination of gel fraction and polymer volume fraction Experimental gel fraction was determined from a leaching study. As-prepared gel sample (thickness ~ 1 mm) was dried at 40 °C for at least 3 days until it reached a constant weight M_0. After that, the sample was immersed in Milli-Q water to let the sol part leach out of the gel network. Water was changed every three hours for 3 times. After that the gel sample was dried completely at 40 °C until it reaches a weight recorded as M. The gel fraction was calculated from the weight after and before the leaching experiment, subtracting the weight (M_s) of initiator, catalyst, and ligand:

$$Gel\ Fraction = \frac{M}{M_0 - M_s} \times 100\ \% \quad (1)$$

Finally the sample was again soaked in Milli-Q water for more than 48 h and the equilibrium weight was recorded as M_t. The polymer volume ratio of the fully swollen gel ($v_{2,s}$) was determined as:

$$v_{2,s} = \frac{V_{2,s}}{V_t} \approx \frac{M/\rho_{PEG2k}}{M_t/\rho_{H_2O}} \quad (2)$$

where $V_{2,s}$ and V_t are volume of polymer and gel, respectively, ρ_{PEG2k} and ρ_{H_2O} are density of PEG2k polymer and H_2O, respectively. Each value was the average of 3 measurements of different samples.

NMR mesurement. ^1H pulsed NMR experiments were performed on a Bruker Minispec MQ-60 spectrometer operating at a proton resonance frequency of 60 MHz. All experiments were performed on the D_2O swollen samples at 309 K. The dead time was 11.1 μs. The lengths of the 90° and 180° pulses were about 1.82 μs and 3.84 μs, respectively. A Hahn echo pulse sequence (HEPS), $90°_x - t_{He} - 180°_y$ – [acquisition of the amplitude of an echo maximum $A(t)$], was used to record the fast part of the T_2 relaxation decay for the rigid component (polymer

chains). t_{He} was varied between 100 μs and 200 ms. At this range, the contribution of solvent (D_2O, $T_2 \sim 2s$) was shielded. A recycle delay of 300 ms was used.

Tensile measurement. The tensile measurements were performed on a dumbbell shape sample (JIS-K6251-7: length 35 mm, width 2 mm, gauge length 12 mm, thickness 0.5-1.5 mm) using a mechanical testing apparatus (Autograph AG-X plus; SHIMADZU, Kyoto, Japan) equipped with a 10 N load cell at a crosshead speed of 10 mm/min. The elongation ratio λ was determined as the deformed length l related to the original length l_0, $\lambda = l/l_0$. The nominal stress σ was estimated as $\sigma = F/A_0$, where A_0 was the cross-section area of the gel sample before deformation, and F the stretching force.

Rheology test. Rheology measurements were performed on an ARES rheometer (advanced rheometric expansion system, Rheometric Scientific Inc.) with a parallel-plate geometry. The test was operated in strain-controlled mode at a shear strain of 0.5%. The disc-shaped samples with a thickness of ~ 3 mm and diameters of 15 mm were used in the test.

FT-IR measurement. IR spectra of dried click gels were obtained at 25 °C on a Bruker Vector 22 IR spectrometer after dispersed in a KBr pellet. A typical spectrum for PEG-2k-azide and G4-20 gel is shown in Fig. S2. The near absence of azido absorbance peak at about 2098 cm^{-1} suggests the near completion of cross-linking reaction.

SIMULATION

Simulation model. In our previous study the model to build an ideal network from an "explosion-contraction" Monte Carlo (MC) algorithm was successfully applied to study the molecular geometry of click gels.[44] In this work, the algorithms, with a modification, is employed to build a randomly defected gel network. Although the off-lattice 3-D MC model

requires more computation time, it is considered to be able to reflect the network structure in space more accurately than previous lattice models.[45,46] A brief summary of the algorithm is introduced in the supporting information.

Determination of gel fraction and elastic fraction. A Spanning Forest of a Graph (SPANFO) algorithm[47] based on graph theory is applied to extract gel parts in the network, by finding the nodes that belong to the largest cluster in the network. Thus the gel fraction (of chain) can be easily calculated as the fraction of chains whose both ends are built in gel part p_g (%) = N_g/N_t, where N_g and N_t are the numbers of nodes belonging to the gel part and total nodes in the network, respectively.

After that, a "Burning Method"[48] is applied to extract elastically effective part that sustains force when the gel network is under deformation. The elastically effective nodes in the network are determined by setting fires from two nodes as near as possible to the diagonal. The approach is in analogy to measure the electric conductivity of the resistor network, as proposed by De Gennes.[49] The method was explicitly described in the reference.[48] When the fire is set for the first time between two nodes, all the paths are "burned"; for the second time, only the shortest path between the two nodes is burned. The path is called the elastic backbone; for the third time, other paths have the same length as the elastic backbones are burned. Those paths are called the growing backbone. Thus all the nodes in the elastic backbone is found. The elastic fraction p_e is defined as the percentage of elastically effective nodes to the total nodes, p_e (%) = N_e/N_t, where N_e and N_t are the numbers of elastic and total nodes in the network, respectively. In the same manner with gel fraction, the elastically effective chain is determined as only those chains with two elastically effective nodes at both ends. The burning method is able to separate the elastic part from inelastic ones such as dangling ends, loops and sol parts as illustrated in Fig. 1. It is

noted that for the reason that a coarse-grained spring model of polymer chain is assumed, we are not able to introduce primary loops(loops that consist only one chain) into the network. We consider this simplification acceptable because the primary loops are shown to take only a small portion (~ 5 %) in the network consisting of 50-mer polymer chains in previous simulation studies.[50]

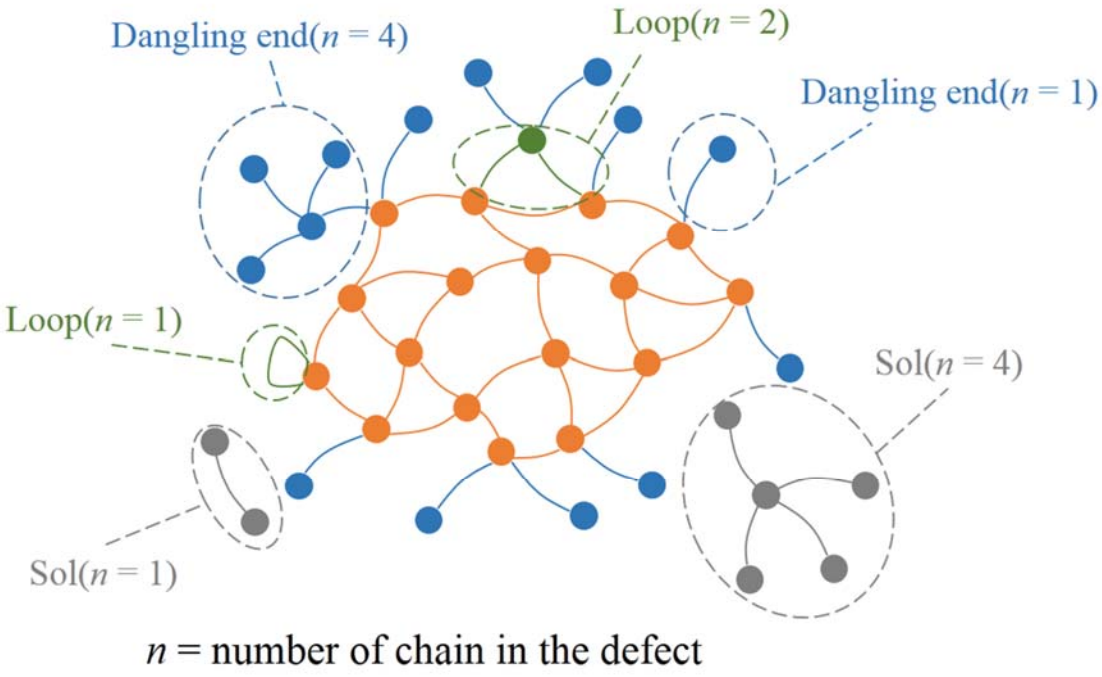

Figure 1. Illustration of topological defects in G4 network.

RESULTS AND DISCUSSION

Network structure analysis. The gel fraction obtained from leaching experiment is plotted against the dangling end percent in Fig.2a. The gel fraction decreases with the increase of defect percentage. For comparison, the simulated result obtained by SPANFO algorithm analysis on the network is also shown in the figure. As shown in Fig. 2a, the experimental gel fraction can be

finely predicted by the simulation, with a minor downturn due to a little of impurity of chemicals and incomplete cross-linking reaction. Overall, G3 network has a lower gel fraction than G4, confirming that the dangling ends have a tremendous effect on integrity for polymer network with low functionality. In both G3 and G4, gel fraction remarkably declines with the defect percent, suggesting that the dangling ends have a large effect on network integrity. The gel fraction of G3 decreases more rapidly than G4, indicating that the defect has a large impact on the integrity of low-functional networks.

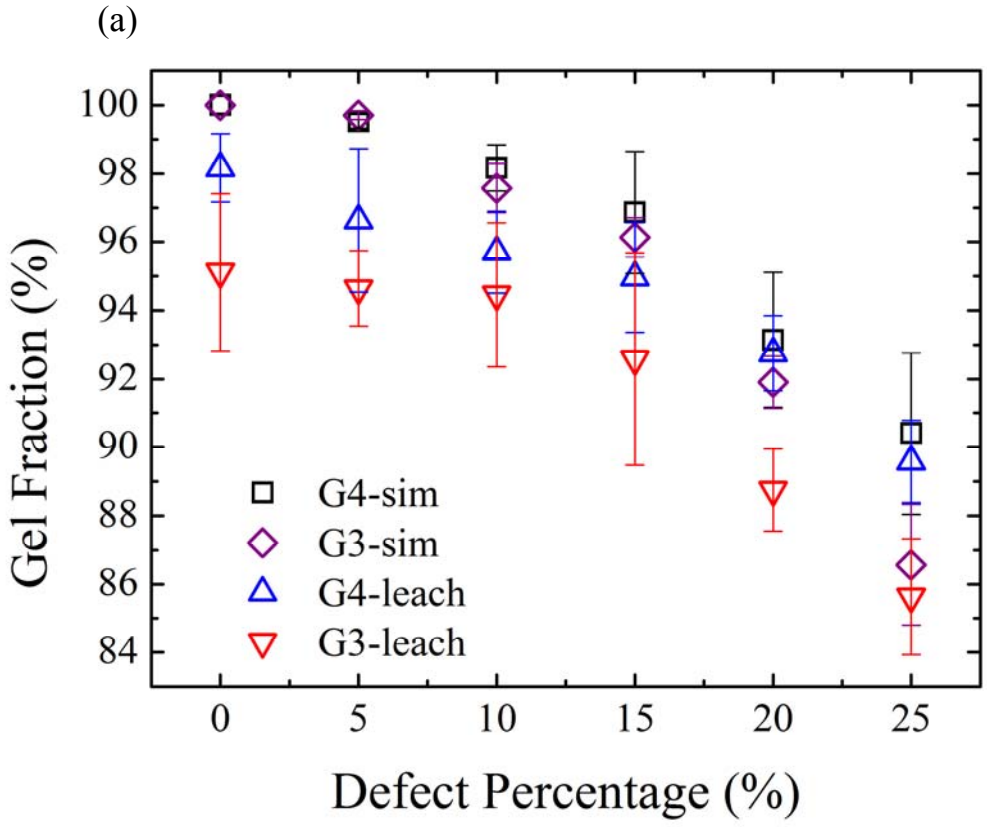

(b)

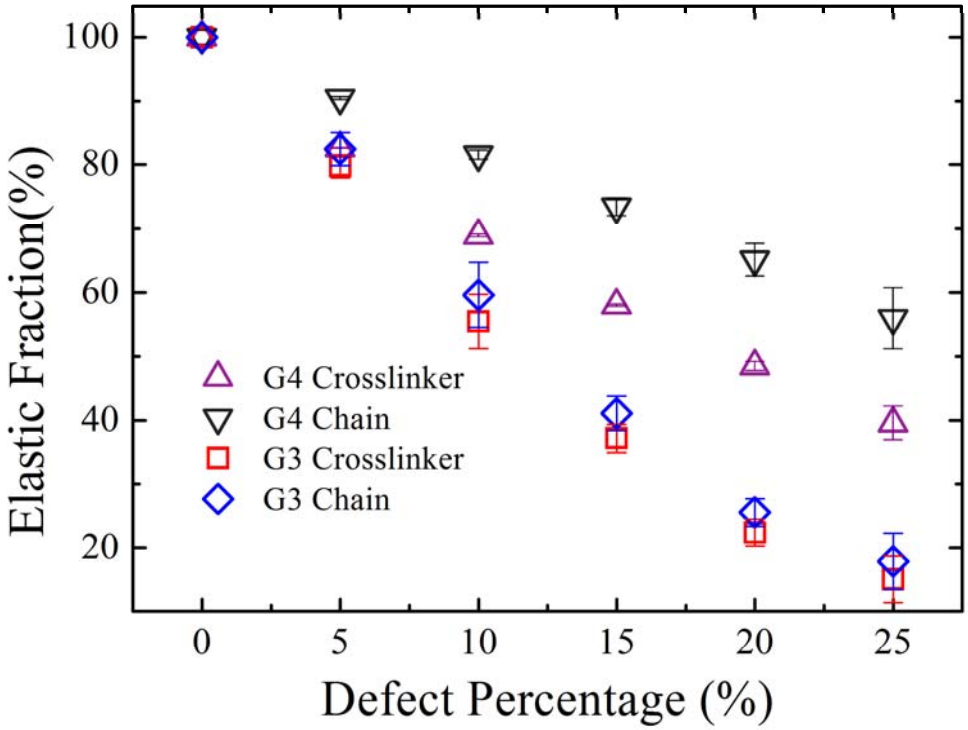

Figure 2. (a) Experimental and simulated gel fraction; (b) Simulated elastic percent of polymer chain and cross-linker.

The elastic percentage in polymer network, referring to those cross-linkers or polymer chains that sustain and transmit force when the network is under deformation, is calculated from "Burning Method" analysis of the defected network described previously. As illustrated in Fig 2(b), the elastic percentage of both cross-linkers and polymer chains of G3 has a larger slope than those of G4. As a result, at a relative large defect percentage, such as 15 %, the elastic percentage of polymer chain in G3 (41 %) is only about half of that in G4 (73 %). This indicates that dangling ends defect has a larger effect upon elastic percent for networks with a lower functionality. For example, at 25 % defect percentage, although the network integrity still remains (gel fractions are ~ 90 % for G4 and 86 % for G3), the elastic percentage is substantially

decreased (56 % for G4 and 18 % for G3), indicating that elastic percentage is more sensitive to the defect than gel fraction. The elastic percentage of both cross-linker and polymer chain can be readily used to calculate elastic cross-linker density ν and elastic chain density μ, which will eventually be used to estimate the modulus of gels and will be discussed below. It should be noted that the elastic percentage calculated from the widely used tree-like Miller-Macosko theory[51,52] is evidently smaller than that calculated from "Burning Method", for the previous theory argued that elastic cross-linkers should have a functionality $f > 2$, while in "Burning Method", the cross-linkers with $f = 2$ can also be elastically effective.

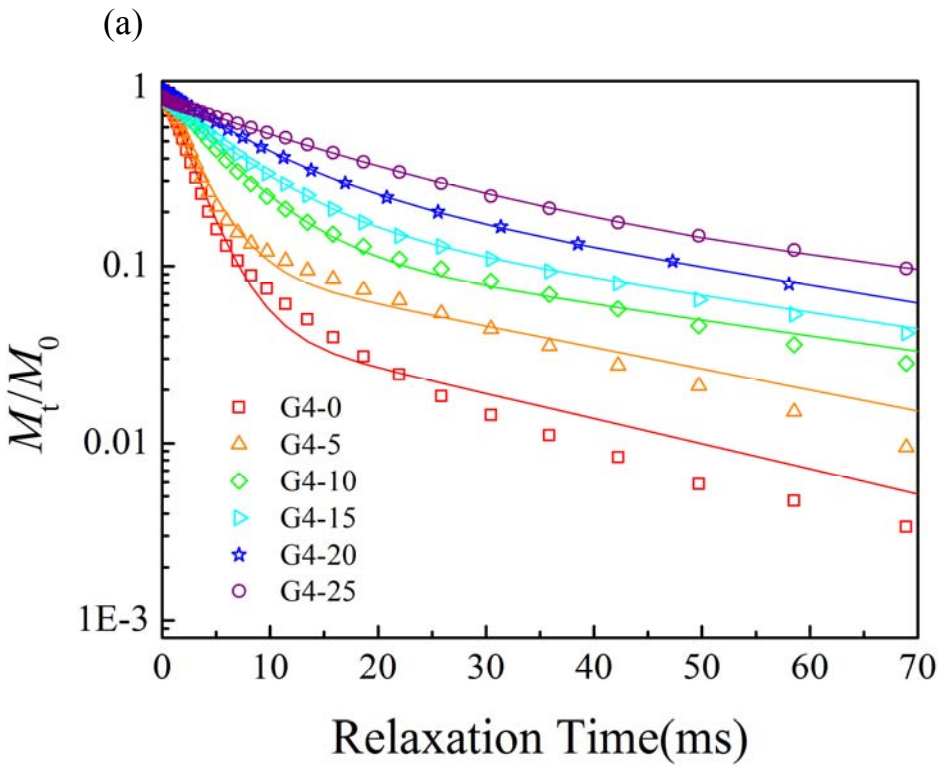

(b)

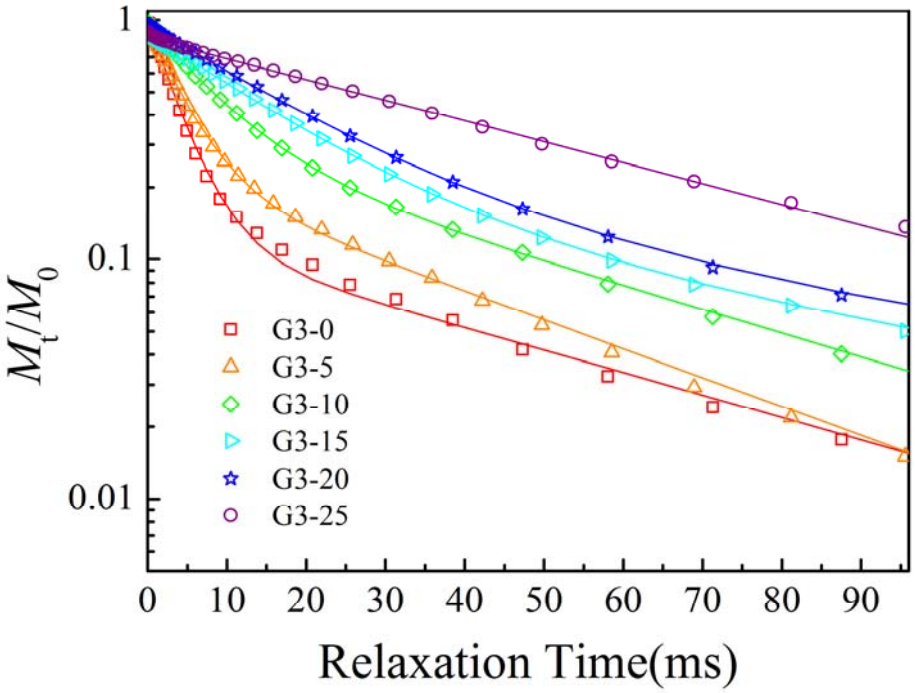
1
0.1
0.01
M_t/M_0
G3-0
G3-5
G3-10
G3-15
G3-20
G3-25
0
10
20
30
40
50
60
70
80
90
Relaxation Time(ms)

1

(c)

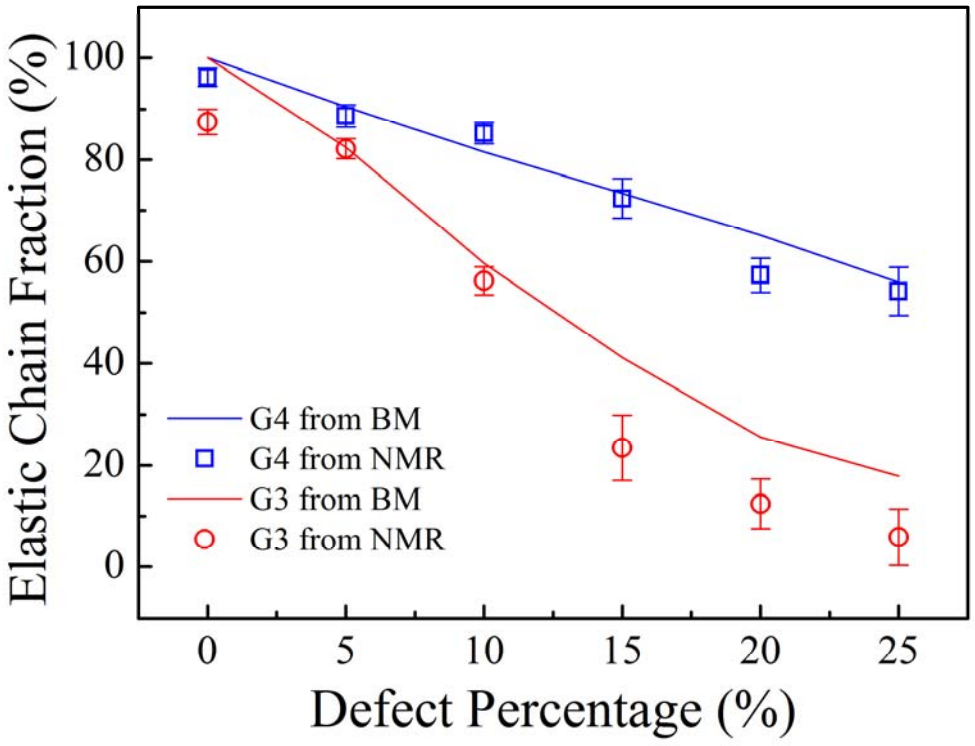
Elastic Chain Fraction (%)
100
80
60
40
20
0
G4 from BM
G4 from NMR
G3 from BM
G3 from NMR
0
5
10
15
20
25
Defect Percentage (%)

2

Figure 3. Transverse relaxation data of (a) G4 series, (b) G3 series (solid line: fit from Eq. (3)); (c) Elastic chain fraction obtained from NMR experiment and Burning Method (BM) calculation.

The experimental elastic percentage was obtained from the low-field NMR experiment. In transverse relaxation experiment, the rigid parts of polymer network (elastic chains) undergo more restriction, resulting in a short T_2 relaxation time. Soft parts including dangling ends, loops and sols have long T_2 relaxation time.[34,53] The T_2 decay curve, illustrated in Fig. 3, was found to be well described by the following equation, consisting of the sum of two exponential models.

$$\frac{M(t)}{M_0} = A_E exp\left(-\frac{t}{T_{2E}}\right) + A_D exp(-\frac{t}{T_{2D}}) \quad (3)$$

where t is the relaxation time, A_E and A_D are amplitudes of elastic and inelastic chain component at time zero, respectively; T_{2E} and T_{2D} are T_2 decay constants of elastic network chain and inelastic network chain, respectively. The elastic chain fraction can be calculated from p'_e (%) = $A_E/(A_E+A_D)$. In Fig. 3(c), the elastic chain fractions obtained from NMR were compared to the values calculated from "burning method". They were in good agreement, confirming the success of introducing precise amount of dangling end defect and the feasibility of simulation method.

Mechanical behavior analyses. The dynamic shear modules G' of these gels were nearly independent of frequency, confirming the elastic character of these chemically cross-linked gels. A typical plot of G', G'' with frequency for G4-20 is shown in Fig. S3. The experimental tensile stress-strain curves of G4 series and G3 series samples are shown in Figure 4. The data of G3-25 was not shown since when the defect percentage was 25 %, the G3 sample was too weak to measure the mechanical properties. All of the tensile stress-strain curves are found to be well

fitted by the Gent model which is widely used to describe stress-strain curve of elastic materials:[54,55]

$$\sigma = G\frac{\lambda_1-\lambda_1^{-2}}{1-(J_1/J_m)} \quad (4)$$

where G is the shear modulus, $J_1=\lambda_1^2+2\lambda_1^{-1}-3$, is the first stress invariant for simple extension in the 1-direction, $\lambda_1 = \lambda$ is the principal stretch ratio in the 1-direction, and J_m is an adjustable parameter representing finite extensibility as a maximum allowable value for the first stress invariant, $J_m = \lambda_m^2+2\lambda_m^{-1}-3$. λ_m is the maximum deformation ratio.

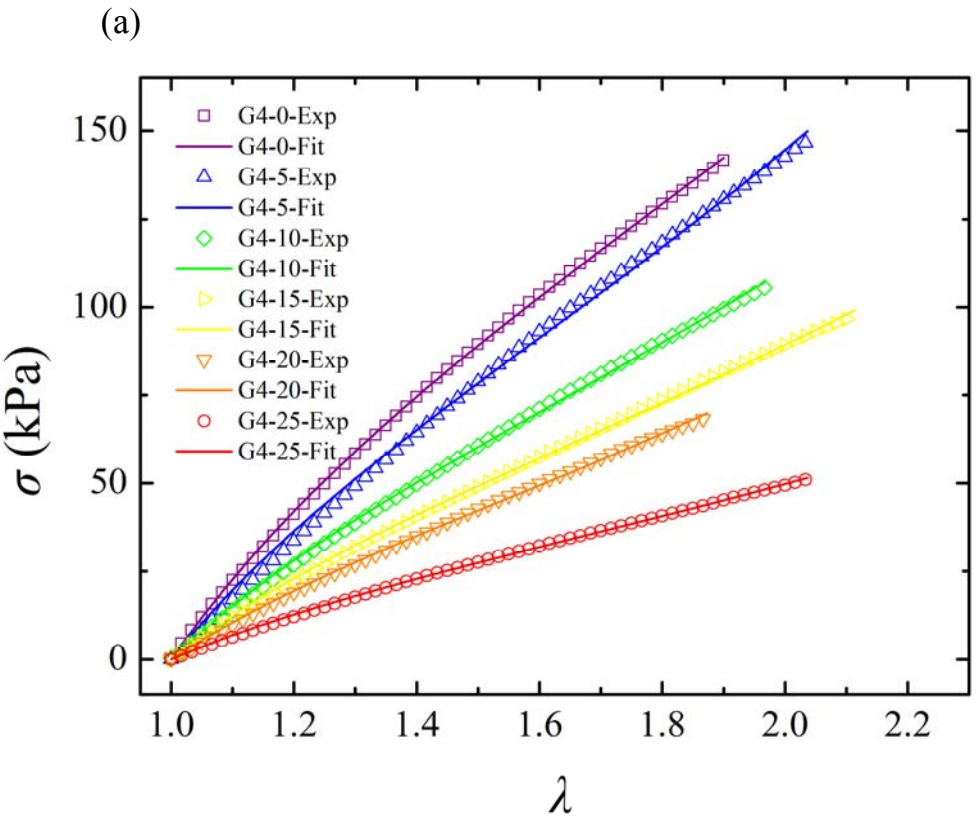

(b)

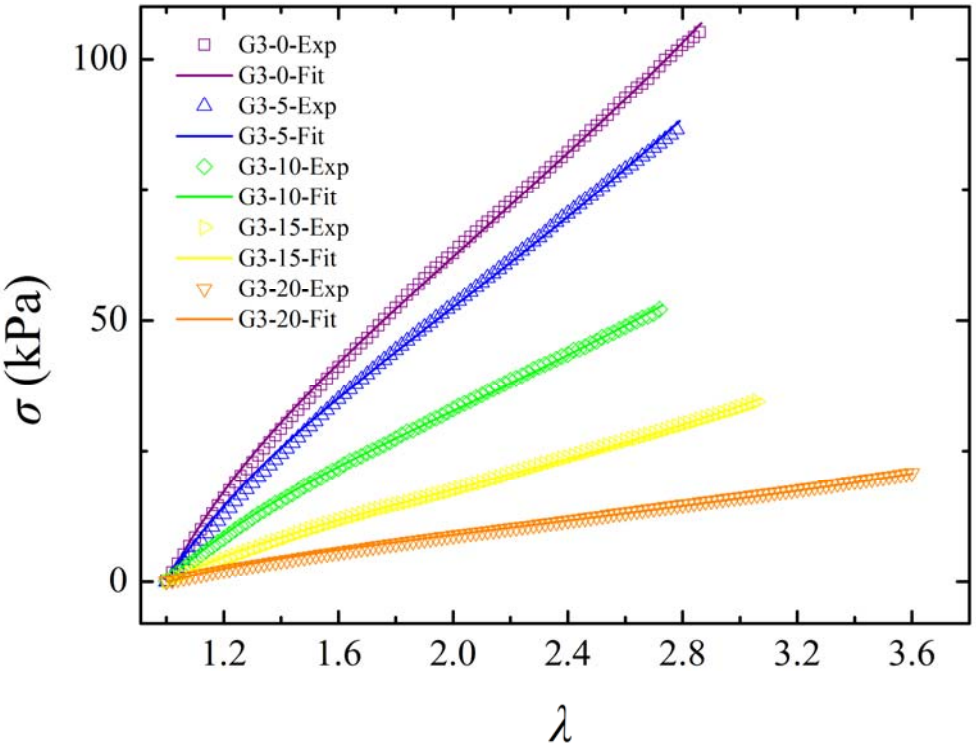

Figure 4. Gent fitting of defected gels. (a) G4 series, (b) G3 series.

The fitting parameters G, J_m and λ_m based on an average of at least 3 samples' stress-strain data are shown in Table 1. The orders of G falls in between few and few tens of kPa, which is about one order of magnitude larger than that of conventional gels with similar chemical structures prepared from free-radical polymerization.[56] When prepared at a similar pre-polymer concentration, G of the defect-free G4 click gel has the same order of magnitude with that of the tetra-PEG gel. The latter was demonstrated to have a very homogeneous network structure.[57] This indicates that the click chemistry offers an alternative method to build well-controlled model networks. G obtained from Gent model fitting is found to be able to precisely predict the shear modulus G' in the rheology test.

As shown in Figure 4, the observed fracture strains of the gels are much lower than the maximum deformation ratio λ_m estimated from the Gent model. In agreement with this, the strain hardening (upturn of slope) effect attributed to the finite extensibility assumption of polymer chain is not observed.[26] This is the result of the brittle nature of the elastic single network gels, which does not dissipate energy during deformation. So, once a few shortest chains are broken, the crack propagates rapidly without showing the finite extensibility behavior and strain hardening in the global stress-strain curves.[58]

Table 1. Fitting parameters of the samples shown in Fig. 4. Each set of data are the averages from at least 3 samples' stress-strain data.

Sample	G/kPa	J_m	λ_m	Sample	G/kPa	J_m	λ_m
G4-0	82.6 ± 1.5	27.5 ± 5.2	5.4 ± 0.5	G3-0	33.9 ± 4.3	43.3 ± 7.4	6.7 ± 0.6
G4-5	71.3 ± 2.8	14.2 ± 6.2	4.0 ± 0.8	G3-5	28.5 ± 4.5	34.1 ± 8.3	6.0 ± 0.7
G4-10	55.0 ± 3.0	14.8 ± 2.4	4.2 ± 0.3	G3-10	17.8 ± 1.0	41.2 ± 1.4	6.6 ± 0.1
G4-15	45.1 ± 0.7	20.7 ± 6.2	4.8 ± 0.6	G3-15	9.5 ± 2.0	63.4 ± 18	8.0 ± 1.2
G4-20	38.5 ± 3.4	13.0 ± 4.7	3.9 ± 0.6	G3-20	5.0 ± 1.0	66.2 ± 14	8.2 ± 0.9
G4-25	25.0 ± 3.6	16.2 ± 6.7	4.2 ± 0.8	G3-25	-	-	-

G*f*-X: *f* = functionality of cross-linkers; X = defect percentage.

(a)

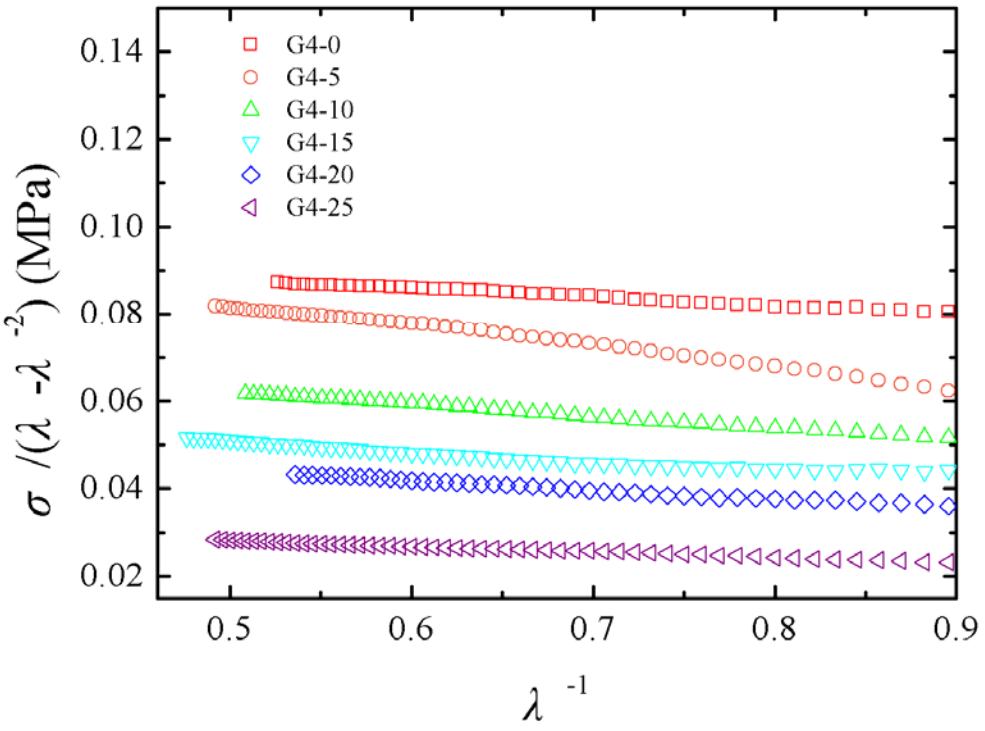
G4-0
G4-5
G4-10
G4-15
G4-20
G4-25
0.14
0.12
0.10
0.08
0.06
0.04
0.02
0.5
0.6
0.7
0.8
0.9
σ /(λ -λ -2) (MPa)
λ -1

1

(b)

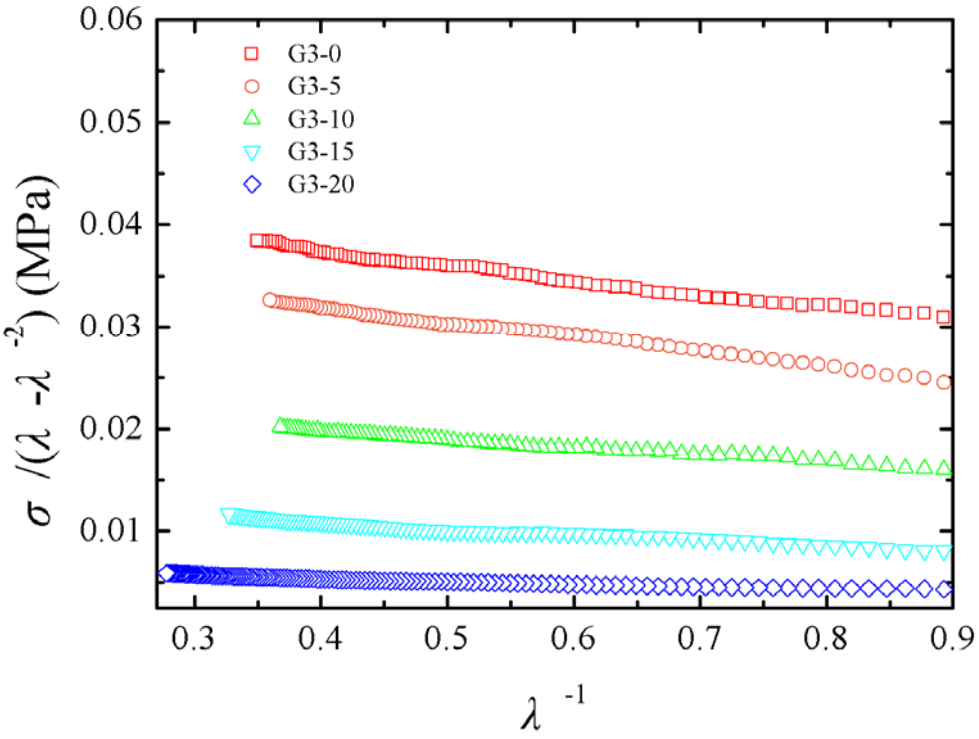
G3-0
G3-5
G3-10
G3-15
G3-20
0.06
0.05
0.04
0.03
0.02
0.01
0.3
0.4
0.5
0.6
0.7
0.8
0.9
σ /(λ -λ -2) (MPa)
λ -1

2

(c)

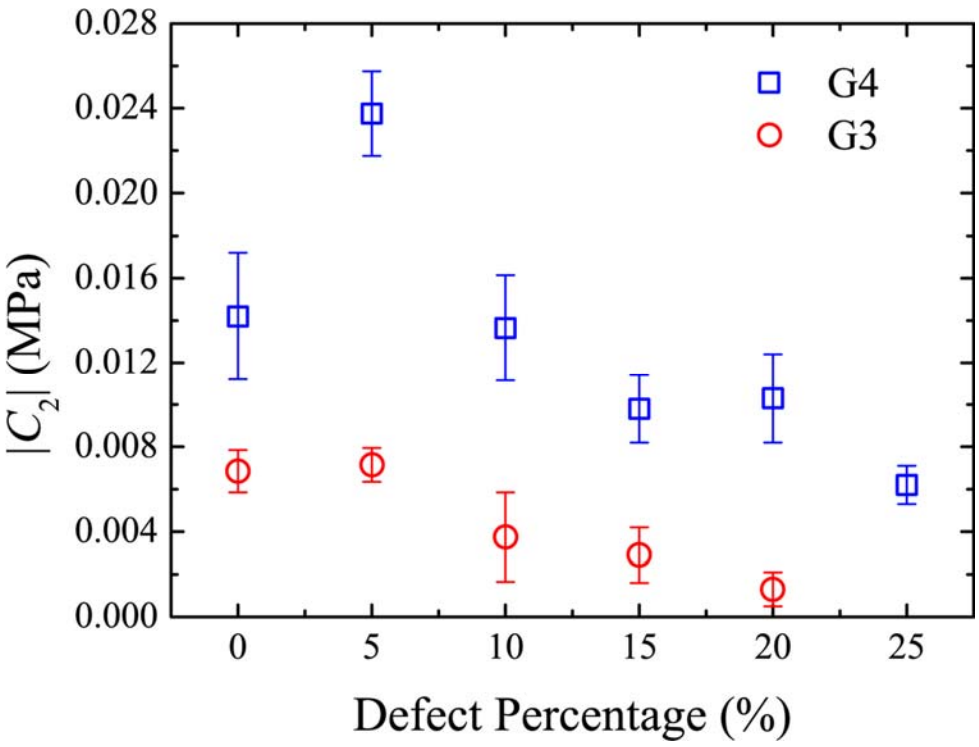

Figure 5. Mooney plot for defected gels (a) G4 series, (b) G3 series and (c) constant C_2 in Mooney-Rivlin model for G4 and G3 series.

To discuss the strain-hardening behavior in more detail, we further analyzed the data in Figure 4 by using the phenomenological Mooney-Rivlin model:

$$\frac{\sigma}{\lambda - 1/\lambda^2} = 2C_1 + \frac{2C_2}{\lambda} \quad (5)$$

where C_1 and C_2 are material constants. $2C_1 = G$ and C_2 is related to strain softening ($C_2 > 0$) or hardening ($C_2 < 0$).

In Fig. 5(a,b), $\sigma/(\lambda\text{-}1/\lambda^2)$ is plotted against $1/\lambda$. For both G4 and G3 series, in all range of strain, C_2 is almost constant and $C_2 < 0$. The phenomenon reveals that very weak strain hardening, originating from finite extensibility of PEG chain, takes effect during the whole test. In Fig. 5(c), the absolute value of C_2, calculated from the slope of Mooney plot in the range of $\lambda^{-1} < 0.9$ is

plotted with defect percentage for both G4 and G3 series. In general, G4 series have a larger $|C_2|$ than that of G3 series, which reflects a relatively prominent finite chain extensibility of G4 network. It can be explained by the more constraint of network chain due to the higher functionality of cross-linkers. In a similar way, a high defect percent renders the network more freedom and less finite chain extensibility effect, leading to a decrease in $|C_2|$ value with the increase of defect percentage for both G4 and G3 series.

Next, we compare the shear modulus G obtained from Gent model fitting to the theoretical value of rubber elasticity models. The most widely used models to describe the elastic modulus of hydrogels are Affine model[59] and Phantom model,[60] where Affine model assumes that cross-linkers are fixed in the network and Phantom model permits the cross-linkers to fluctuate in space under network deformation. Previous works have argued that at most time the well-defined single network gels follow the Phantom model prediction.[43,61] Click gels with controlled dangling end defect also support this argument, which will be shown as follows.

For Phantom model, modules can be calculated as $G = (\nu\text{-}\mu)RT$, where ν and μ are the number density of elastically effective chain and cross-linkers, respectively. R is the gas constant and T is absolute temperature. In this model, precise estimation of ν and μ is necessary. In this study, ν and μ are both calculated from a combining swelling and "burning method" analysis. $\nu = c_\nu p_\nu$ and $\mu = c_\mu p_\mu$. Here, $c_\nu = m_0 N_A / M_s V_t$ is the number density of PEG2k chain in swollen gel obtained from the swelling data, where m_0 is the weight of the pre-polymer; $c_\mu = c_\nu/(f/2)$ is the number density of cross-linkers in swollen gel, where f is the functionality of the cross-linker (f=3, and 4 for G3 and G4, respectively) . p_ν and p_μ are elastic percentages of polymer chains and cross-linkers, respectively, which are calculated by "Burning Method" analysis on the network. As shown in Fig. 6, the experimental modulus with various defect percentage are well predicted

by Phantom model, indicating there exist few trapped entanglements at low deformation region for all samples, which is usually believed to be the main cause for a larger modulus than Phantom prediction. The result is in consistent with that of the Tetra-PEG gels prepared at c^*, which is demonstrated to be a homogeneous network by SANS characterization.[43] We note that the slight downturn at small defect percentage (0 % - 10 %) may result from the impurity of PEG2k-azide.

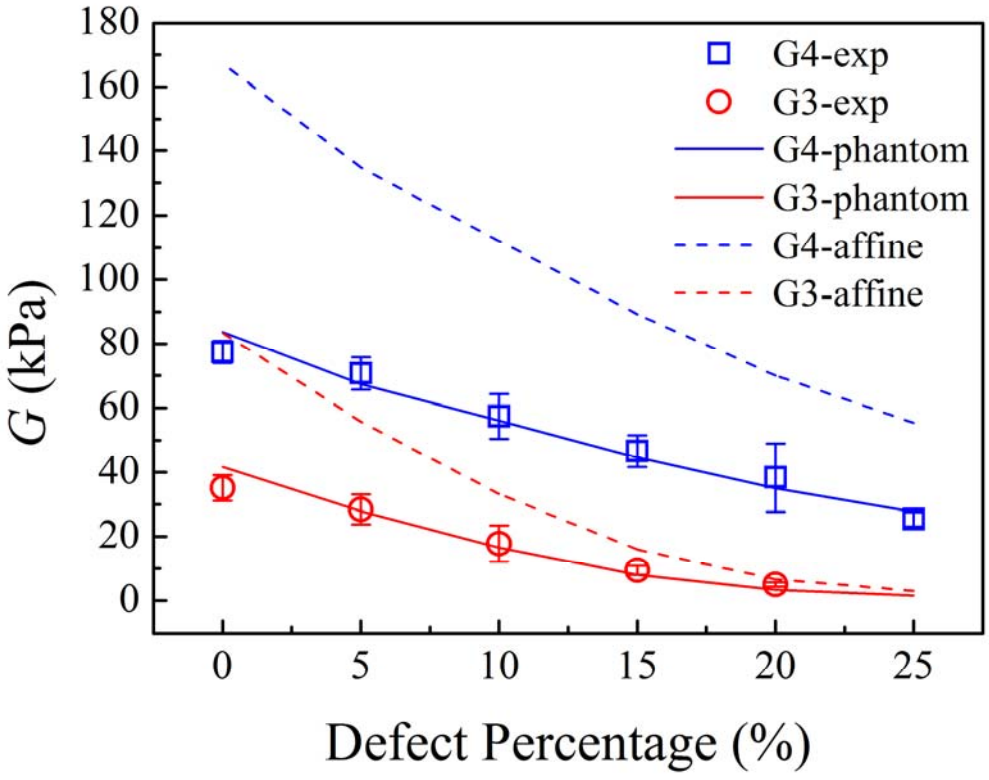

Figure 6. Shear moduli of gels with various defects observed by experiment, and predicted by Affine and Phantom models.

Further, we compare the maximum extension ratio λ_m obtained from the Gent model fitting with the theoretical value obtained from Affine model and Phantom model. λ_m from the Gent model fitting parameters rather than the observed deformation ratios at fracture in the tensile test is studied because the former represent the average finite extensibility of polymer chains, while the latter is dominated by several shortest chains that initiate the global fracture.

If the affine behavior is applied, the cross-linking points are fixed in space and polymer chains deform affinely with the network, both G4 samples and G3 samples should have the same λ_m. By affine assumption, λ_m of click gel with M_c = 2100 g/mol can be predicted using the Kuhn model:[62]

$$\lambda_m = \frac{L}{R_0} = \frac{bN_e}{bN_e^{\nu 1}} \quad (6)$$

where L and R_0 are the contour length and unstretched end-to-end distance of PEG2k chain, respectively. L can be calculated from the Kuhn length for PEG (0.76 nm) and the effective number of Kuhn segments (N_e = 21.7 for PEG2k).[63] R_0 varies with the scaling exponent ν_1, based on which state is the chain in before deformation. For Gaussian chain, ν_1 = 0.5; for a self-avoiding polymer chain in a good solvent, ν_1 = 0.6; for a self-avoiding chain in two dimensions, ν_1 = 0.75; for a fully extended chain, ν_1 = 1.0.[56] Thus when we assume a Gaussian chain, $\lambda_m = N_e^{1-0.5} = 4.65$; for a self-avoiding chain in good solvent, which is more suitable for our system, $\lambda_m = N_e^{1-0.6} = 3.42$.

If the phantom behavior is applied, the cross-linking points fluctuate in space and λ_m depends on the functionality of cross-linkers. By Phantom assumption, a fluctuating chain consisting of N monomers can be considered as a non-fluctuating chain consisting of $Nf/(f-2)$ monomers. Thus λ_m can be estimated as:

$$\lambda_{m(Phantom,f=4)} = 2\lambda_{m(Affine,f=4)}$$

$$\lambda_{m(Phantom,f=3)} = 1.5\lambda_{m(Affine,f=3)} \quad (7)$$

In Fig. 7, λ_m obtained from Gent model fitting is plotted against defect percent. For comparison, the results estimated from the affine model and Phantom model for network of functionality of 3 and 4 are shown using $v_1 = 0.6$.

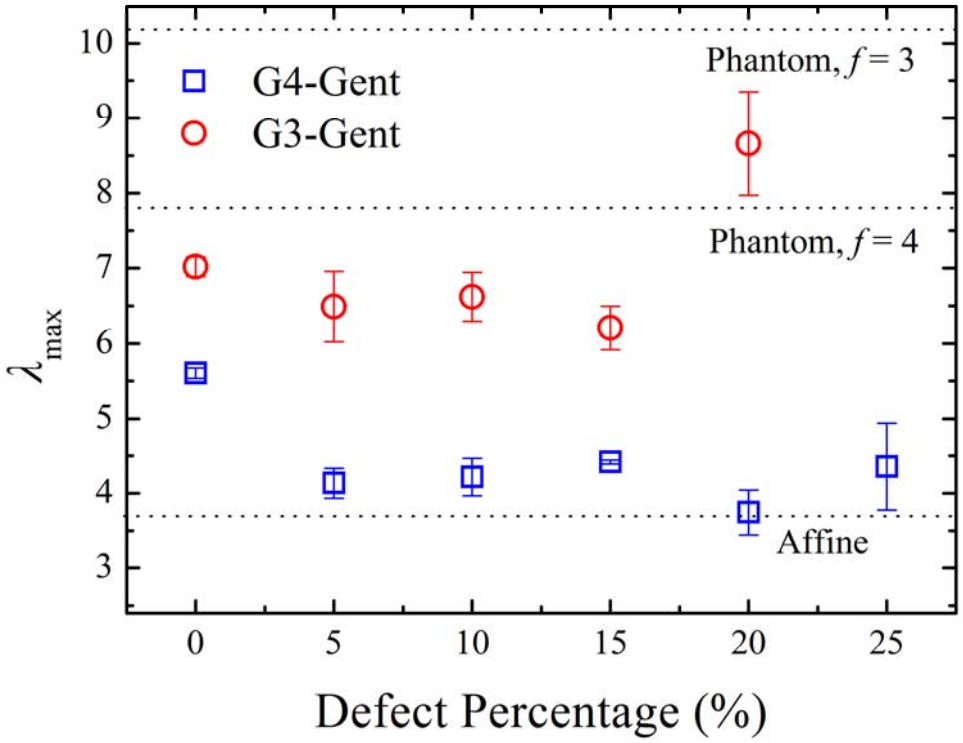

Figure 7. Maximum extension ratio vs defect percentage for G3 and G4. The dotted lines show the theoretical value estimated from Phantom or Affine models.

The λ_m obtained from the Gent model fitting showed values between that from the Affine model and Phantom model. This result indicates that at large deformation, the fluctuation of cross-linking points is suppressed for some extend but still exists. The result that the G3 series gels have a relatively large λ_m than that of the G4 series also indicates the existence of the

fluctuation effect of cross-linking points. Except for the G3 sample of 20% defect percentage, the λ_m obtained from the Gent model fitting was slightly reduced by the introduction of defects. For G3-20, λ_m abruptly increase to 8.6, by increasing the freedom of cross-linker fluctuation.

Polymer volume fraction. The Flory-Rehner model[59] predicts swelling behavior based on the assumption of additivity of the free energy of mixing and the free energy of elasticity. For Phantom network, polymer volume fraction can be predicted by:[64]

$$\ln(1 - v_{2,s}) + v_{2,s} + \chi v_{2,s}^2 = -v_1(\nu - \mu)v_{2,s}^{1/3} \quad (8)$$

where $v_{2,s}$ is the polymer volume fraction at equilibrium swelling, χ is the polymer-solvent interaction parameter (0.426 for PEG-water system[65]), v_1 is the molar volume of the solvent (18 L/mol), ν and μ are number density of elastically effective chain and cross-linkers in dry gel, respectively. It is noted that recent studies argue that χ varies with the polymer volume fraction, while a relatively stable value of χ is observed in polymer network at a polymer volume fraction of 0-0.2,[66] which is the case in our system. Thus a constant χ is a reasonable simplification applied in this study.

Based on $\nu - \mu$ estimated from the "Burning Method", $v_{2,s}$ can be readily predicted. Fig. 8 illustrated the predicted and experimental polymer volume fraction. As defect percentage increases, $v_{2,s}$ decreases, as the dangling parts in network contributes to the free energy of mixing and not to the free energy of elasticity. Overall, the experimental $v_{2,s}$ are well predicted by Flory-Rehner theory except for the minor discrepancy at low defect percentage, which may be resulted from the impurity of click materials and limitation in application of Flory-Rehner model in a inhomogeneous system.[67]

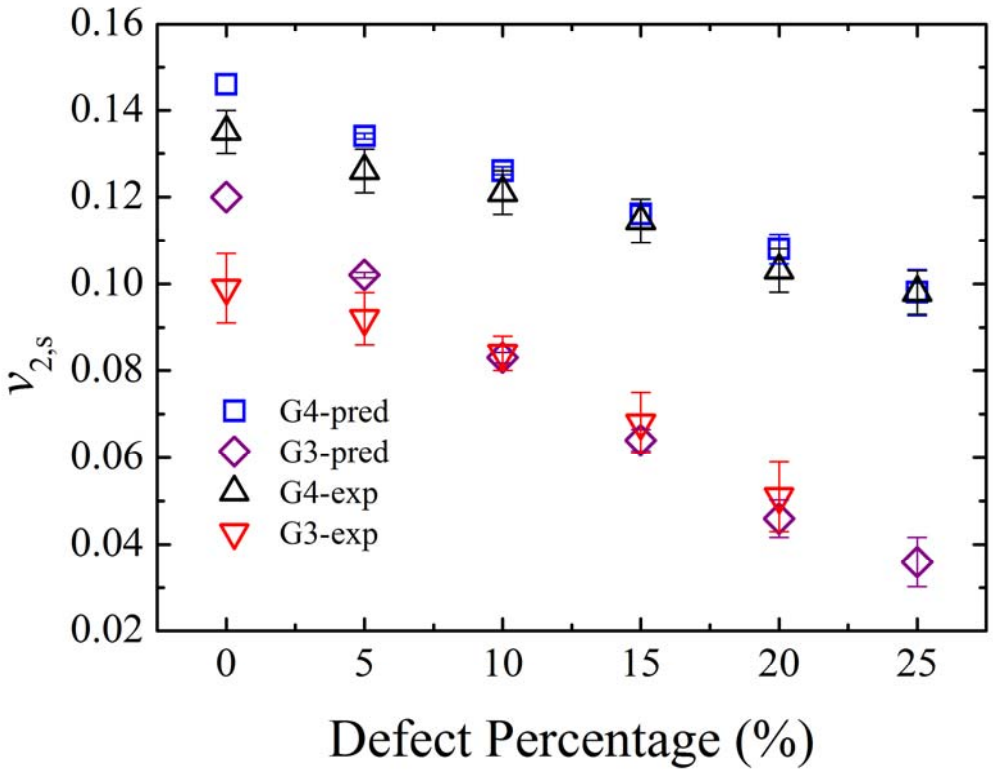

Figure 8. Polymer volume fraction $v_{2,s}$ against the defect percentage obtained from experimental observation and from prediction of Flory-Rehner model.

CONCLUSION

In this work we proposed, to the best of our knowledge, the first attempt to control gel properties with the help of dangling ends defect. A method based on click chemistry was demonstrated to introduce precise amount of dangling ends in polymer gels. The network structure was confirmed by low-field NMR characterization and Monte Carlo simulation. The shear modulus and polymer volume fraction were well predicted by Phantom model, indicating the discrepancy from Affine assumption in swollen chemical gels. Discussion of maximum extension ratio revealed that the fluctuation of cross-linkers was enhanced by either decreasing

network functionality or increasing dangling ends. The study showed the potential of combined click chemistry and Monte Carlo simulation in design of hydrogel materials with precise properties and the study of rubber elasticity. More extensive work based on the combined method is on the way.

AUTHOR INFORMATION

Corresponding Author

* School of Chemistry and Chemical Engineering, Southeast University, Jiangning District, Nanjing, Jiangsu Province, P. R. China 211189. Tel.: +86-25-52090625; Fax: +86-25-52090625. Email: fu7352@seu.edu.cn (G. D. Fu)

* Faculty of Advanced Life Science, Hokkaido University, Sapporo, 060-0810, Japan Email: gong@mail.sci.hokudai.ac.jp (J. P. Gong)

ACKNOWLEDGMENTS

A. K. Zhang thanks Dr. Rongsheng Lu and Dr. Kay Saalwächter for fruitful discussion on NMR experiment. This work was supported by National Natural Science Foundation of China (Grant No. 21274020, 21074022 and 21304019) and Zhejiang Provincial Natural Science Foundation of China (No. Y4110115). This work was also partially supported by a Grant-in-Aid for Scientific Research (S) (No. 124225006) from the Japan Society for the Promotion of Science (JSPS).

REFERENCES

1. E. S. Place, J. H. George, C. K. Williams, M. M. Stevens. *Chem. Soc. Rev.* **2009**, 38, 1139-1151.
2. J. L. Drury, D. J. Mooney. *Biomaterials* **2003**, 24, 4337-4351.
3. P. Gupta, K. Vermani, S. Garg. *Drug Discovery Today* **2002**, 7, 569-579.
4. Y. Qiu, K. Park. *Adv. Drug Deliv. Rev.* **2001**, 53, 321-339.
5. B. H. Cipriano, S. J. Banik, R. Sharma, D. Rumore, W. Hwang, R. M. Briber, S. R. Raghavan. *Macromolecules* **2014**, 47, 4445-4452.
6. M. J. Zohuriaan-Mehr, H. Omidian, S. Doroudiani, K. Kabiri. *J Mater Sci* **2010**, 45, 5711-5735.
7. A. Shikanov, R. M. Smith, M. Xu, T. K. Woodruff, L. D. Shea. *Biomaterials* **2011**, 32, 2524-2531.
8. F. Ikkai, M. Shibayama. *J. Polym. Sci., Part B: Polym. Phys.* **2005**, 43, 617-628.
9. M. Rubinstein, R. Colby. Polymers Physics; Oxford University: Oxford, U.K., 2003.
10. Y. Akagi, T. Katashima, Y. Katsumoto, K. Fujii, T. Matsunaga, U. Chung, M. Shibayama, T. Sakai. *Macromolecules* **2011**, 44, 5817-5821.
11. T. Sakai, T. Matsunaga, Y. Yamamoto, C. Ito, R. Yoshida, S. Suzuki, N. Sasaki, M. Shibayama, U. I. Chung. *Macromolecules* **2008**, 41, 5379-5384.
12. Y. Okumura, K. Ito. *Adv. Mater.* **2001**, 13, 485-487.
13. J. P. Gong, Y. Katsuyama, T. Kurokawa, Y. Osada. *Adv. Mater.* **2003**, 15, 1155-1158.
14. K. Nishi, M. Chijiishi, Y. Katsumoto, T. Nakao, K. Fujii, U.-i. Chung, H. Noguchi, T. Sakai, M. Shibayama. *J. Chem. Phys.* **2012**, 137, 224903.
15. H. C. Kolb, M. G. Finn, K. B. Sharpless. *Angew. Chem. Int. Ed.* **2001**, 40, 2004-2021.
16. R. A. Evans. *Aust. J. Chem.* **2007**, 60, 384-395.
17. L. Q. Xu, F. Yao, G. D. Fu, E. T. Kang. *Biomacromolecules* **2010**, 11, 1810-1817.
18. M. H. Samiullah, D. Reichert, T. Zinkevich, J. Kressler. *Macromolecules* **2013**, 46, 6922-6930.
19. H. Shih, C.-C. Lin. *Biomacromolecules* **2012**, 13, 2003-2012.
20. J. A. Johnson, D. R. Lewis, D. D. Díaz, M. G. Finn, J. T. Koberstein, N. J. Turro. *J. Am. Chem. Soc.* **2006**, 128, 6564-6565.
21. M. Malkoch, R. Vestberg, N. Gupta, L. Mespouille, P. Dubois, A. F. Mason, J. L. Hedrick, Q. Liao, C. W. Frank, K. Kingsbury, C. J. Hawker. *Chem. Commun.* **2006**, 2774-2776.
22. T. J. Sanborn, P. B. Messersmith, A. E. Barron. *Biomaterials* **2002**, 23, 2703-2710.
23. C. Li, M. J. Rowland, Y. Shao, T. Cao, C. Chen, H. Jia, X. Zhou, Z. Yang, O. A. Scherman, D. Liu. *Adv. Mater.* **2015**, 27, 3298-3304.
24. K. Li, C. Zhou, A. k. Zhang, S. Qian, Y. Li, F. Yao, G. D. Fu. **Submitted**.
25. F. Lange, K. Schwenke, M. Kurakazu, Y. Akagi, U.-i. Chung, M. Lang, J.-U. Sommer, T. Sakai, K. Saalwaechter. *Macromolecules* **2011**, 44, 9666-9674.
26. W. Chasse, M. Lang, J. U. Sommer, K. Saalwachter. *Macromolecules* **2012**, 45, 899-912.
27. M. A. Malmierca, A. González-Jiménez, I. Mora-Barrantes, P. Posadas, A. Rodríguez, L. Ibarra, A. Nogales, K. Saalwächter, J. L. Valentín. *Macromolecules* **2014**, 47, 5655-5667.
28. M. Shibayama. *Macromol. Chem. Phys.* **1998**, 199, 1-30.
29. K. Nishi, H. Asai, K. Fujii, Y.-S. Han, T.-H. Kim, T. Sakai, M. Shibayama. *Macromolecules* **2014**, 47, 1801-1809.
30. K. Fujii, H. Asai, T. Ueki, T. Sakai, S. Imaizumi, U.-i. Chung, M. Watanabe, M. Shibayama. *Soft Matter* **2012**, 8, 1756-1759.
31. H. X. Zhou, J. Woo, A. M. Cok, M. Z. Wang, B. D. Olsen, J. A. Johnson. *Proc. Natl. Acad. Sci. USA* **2012**, 109, 19119-19124.
32. K. Kawamoto, M. Zhong, R. Wang, B. D. Olsen, J. A. Johnson. *Macromolecules* **2015**, 48, 8980-8988.
33. P.-D. Hong, J.-H. Chen. *Polymer* **1998**, 39, 5809-5817.
34. K. Saalwächter. *Macromolecules* **2005**, 38, 1508-1512.
35. N. Metropolis, S. Ulam. *Journal of the American Statistical Association* **1949**, 44, 335-341.

36. K. Binder. Oxford University Press, New York, 1995.
37. S. Dutton, R. F. T. Stepto, D. J. R. Taylor. *Angew. Makromol. Chem* **1996**, 240, 39-57.
38. S. Edgecombe, P. Linse. *Macromolecules* **2007**, 40, 3868-3875.
39. S. Edgecombe, P. Linse. *Polymer* **2008**, 49, 1981-1992.
40. M. Gragert, M. Schunack, W. H. Binder. *Macromol. Rapid Commun.* **2011**, 32, 419-425.
41. M. Schunack, M. Gragert, D. Dohler, P. Michael, W. H. Binder. *Macromol. Chem. Phys.* **2012**, 213, 205-214.
42. G. D. Fu, H. Jiang, F. Yao, L. Q. Xu, J. Ling, E. T. Kang. *Macromol. Rapid Commun.* **2012**, 33, 1523-1527.
43. Y. Akagi, J. P. Gong, U. Chung, T. Sakai. *Macromolecules* **2013**, 46, 1035-1040.
44. A. K. Zhang, J. Ling, Y. W. Sun, G. D. Fu. *Chin. J. Polym. Sci.* **2015**, 33, 721-731.
45. M. Laradji, H. Guo, M. J. Zuckermann. *Phys. Rev. E* **1994**, 49, 3199-3206.
46. W. Bruns. *J. Phys. A: Math. Gen.* **1977**, 10, 1963.
47. A. Nijenhuis, H. S. Wilf. In Computer Science and Applied Mathematics, New York: Academic Press, 1978, 2nd ed., 1978.
48. H. J. Herrmann, D. C. Hong, H. E. Stanley. *J. Phys. A: Math. Gen.* **1984**, 17, L261-L266.
49. P. G. D. Gennes. *J. Phys. (France) Lett.* **1976**, 37, L1-L2.
50. N. Gilra, C. Cohen, A. Z. Panagiotopoulos. *J. Chem. Phys.* **2000**, 112, 6910-6916.
51. C. W. Macosko, D. R. Miller. *Macromolecules* **1976**, 9, 199-206.
52. D. R. Miller, C. W. Macosko. *Macromolecules* **1976**, 9, 206-211.
53. H. Luo, M. Klüppel, H. Schneider. *Macromolecules* **2004**, 37, 8000-8009.
54. A. N. Gent. *Rubber Chem. Technol.* **1996**, 69, 59-61.
55. R. E. Webber, C. Creton, H. R. Brown, J. P. Gong. *Macromolecules* **2007**, 40, 2919-2927.
56. D. J. Waters, K. Engberg, R. Parke-Houben, L. Hartmann, C. N. Ta, M. F. Toney, C. W. Frank. *Macromolecules* **2010**, 43, 6861-6870.
57. T. Sakai, Y. Akagi, T. Matsunaga, M. Kurakazu, U.-i. Chung, M. Shibayama. *Macromol. Rapid Commun.* **2010**, 31, 1954-1959.
58. J. P. Gong. *Soft Matter* **2010**, 6, 2583-2590.
59. P. J. Flory. Principles of Polymer Chemistry; Cornell University Press, 1953.
60. H. M. James, E. Guth. *J. Chem. Phys.* **1953**, 21, 1039-1049.
61. S. Schloegl, M.-L. Trutschel, W. Chasse, G. Riess, K. Saalwaechter. *Macromolecules* **2014**, 47, 2759-2773.
62. S. P. Obukhov, M. Rubinstein, R. H. Colby. *Macromolecules* **1994**, 27, 3191-3198.
63. E. M. Saffer, M. A. Lackey, D. M. Griffin, S. Kishore, G. N. Tew, S. R. Bhatia. *Soft Matter* **2014**, 10, 1905-1916.
64. S. K. Patel, S. Malone, C. Cohen, J. R. Gillmor, R. H. Colby. *Macromolecules* **1992**, 25, 5241-5251.
65. L. G. Cima, S. T. Lopina. *Macromolecules* **1995**, 28, 6787-6794.
66. J. L. Valentin, J. Carretero-Gonzalez, I. Mora-Barrantes, W. Chasse, K. Saalwaechter. *Macromolecules* **2008**, 41, 4717-4729.
67. B. Radi, R. M. Wellard, G. A. George. *Macromolecules* **2010**, 43, 9957-9963.